Ultrasonics Sonochemistry 90 (2022) 106188

Contents lists available at ScienceDirect

Ultrasonics Sonochemistry

journal homepage: www.elsevier.com/locate/ultson

Dual improvement in curcumin encapsulation efficiency and lyophilized complex dispersibility through ultrasound regulation of curcumin–protein assembly

Hualin Dong, Peng Wang *, Zongyun Yang, Ru Li, Xinglian Xu, Juan Shen

Key Laboratory of Animal Products Processing, Ministry of Agriculture, Key Laboratory of Meat Processing and Quality Control, Ministry of Education, Jiangsu Synergetic Innovation Center of Meat Production and Processing, and College of Food Science and Technology, Nanjing Agricultural University, Nanjing, Jiangsu 210095, People's Republic of China

ARTICLE INFO

Keywords:
Curcumin
Ultrasound
Nano-complexation
Freeze drying

ABSTRACT

Ultrasound has a recognized ability to modulate the structure and function of proteins. Discovering the influential mechanism of ultrasound on the intramolecular interactions of egg-white protein isolate–curcumin (*EPI*–Cur) nanoparticles and their intermolecular interaction during freeze drying and redispersion is meaningful. In this study, under the extension of pre-sonication time, the protein solubility, surface hydrophobicity, and curcumin encapsulation rate showed an increasing trend, reaching the highest value at 12 min of treatment. However, the values decreased under the followed extension of ultrasound time. After freeze drying and redispersion were applied, the *EPI*–Cur sample under 12 min of ultrasound treatment exhibited minimal aggregation degree and loss of curcumin. The retention and loading rates of curcumin in the lyophilized powder reached 96 % and 33.60 mg/g *EPI*, respectively. However, under excessive ultrasound of >12 min, scanning electron microscopy showed distinct blocky aggregates. Overexposure of the hydrophobic region of the protein triggered protein-mediated hydrophobic aggregation after freeze drying. X-ray diffraction patterns showed the highest crystallinity, indicating that the free curcumin-mediated hydrophobic aggregation during freeze drying was enhanced by the concentration effect and intensified the formation of larger aggregates. This work has practical significance for developing the delivery of hydrophobic active substances. It provides theoretical value for the dynamic dispersity change in protein-hydrophobic active substances during freeze drying and redissolving.

1. Introduction

As a kind of plant polyphenol, curcumin has been thoroughly proven to have various physiological activities. Studies have shown that curcumin could be used as a nutritional supplement in food to enhance the therapeutic effect of gastrointestinal cancer, tumor, inflammation, and other diseases [28,43]. Curcumin has substantial nutritional and medicinal value, but the inherent physical and chemical properties of hydrophobic polyphenols (poor water solubility, low bioavailability, chemical instability, and photodegradation) limit its application. Complexes with food proteins have been considered an effective and facile method to improve the solubility and bio-accessibility of hydrophobic active substances [50,64]. However, liquid complexes are prone to oxidative deterioration, and the prepared protein–curcumin complexes are susceptible to environmental effects and precipitation deactivation, thus limiting their applications. Therefore, protein nanocomplexes must be transformed from liquid to dry powder.

Freeze drying is an essential method for constructing protein nanoparticles [4,7,14,26]. Protein-bioactive nanocomposite powders prepared by freeze drying typically have high encapsulation efficiency (EE) and good re-dispersibility in water, confirming the effectiveness of freeze drying in developing highly water-dispersible protein-hydrophobic active substances [10,12,55]. In addition, freeze-dried phenolics exhibited higher bioactivity and recovery than spray-dried ones [17,36,37,44,60] due to the low thermal stress to which the active substance are subjected [3]. Such phenomenon improved the stability of the core compounds against degradation [1,40,48], and it is fully applied in the encapsulation of high value-added and heat-sensitive

* Corresponding author.
E-mail address: wpeng@njau.edu.cn (P. Wang).

https://doi.org/10.1016/j.ultsonch.2022.106188
Received 16 August 2022; Received in revised form 25 September 2022; Accepted 30 September 2022
Available online 3 October 2022
1350-4177/© 2022 Published by Elsevier B.V. This is an open access article under the CC BY-NC-ND license (http://creativecommons.org/licenses/by-nc-nd/4.0/).

activities.

The freeze-drying process consists of three main steps: freezing, primary drying, and secondary drying [35]. Freezing is mainly a process of ice nucleation, in which the water content within the protein gradually decreases, the tension increases, and the bound water interacting with the protein through hydrogen bonding and van der Waals forces gradually freezes, resulting in the destruction of the protein structure and the exposure of the hydrogen bonding and hydrophobic regions [23,31,46]. The denaturation in the drying process mainly occurs at the stage of removing bound water from the secondary drying. Water molecules surround the surface of the protein in an aqueous solution to form a single molecular hydration layer [11]. This layer of water interacts with proteins through hydrogen bonds. During the drying process, with the sublimation of ice crystals, the protein hydration shell is gradually removed, thus destroying the hydrogen bond structure on the protein surface and making the protein transfer protons to the ionized carboxyl group to reduce its charge distribution [5,49]. A decrease in charge density is beneficial for enhancing protein surface hydrophobicity (H_0), promoting the hydrophobic aggregation of the protein, and even leading to protein denaturation [32,56,59]. Small-molecule phenolic compounds usually bound to proteins through hydrogen bonding and hydrophobic interactions [8,20,24,33]. Hydrophobic interactions are mainly caused by the benzene ring of polyphenols and hydrophobic sites of proteins, such as the pyrrole ring of proline residues. Hydrogen bonding occurs mainly between the hydrogen atom acceptor sites of proteins and the hydroxyl groups of polyphenols. When the hydrophobic pocket of proteins opens, it weakens the electrostatic interactions and enhances the H_0 of proteins, favoring the binding of proteins and polyphenols [68]. Such binding may reduce the hydrophobic aggregation between proteins due to concentration effect. However, when too many free polyphenols are present, they could act as polydentate ligands and become bridging agents for two proteins or polyphenol–protein complexes, gradually forming protein dimers. The more polyphenols are formed, the larger the aggregates are, and precipitation is even formed [39,47,53]. Therefore, the interaction between polyphenols and proteins and the present state of polyphenols in the system may affect the degree of aggregation and denaturation of proteins during freeze drying. To date, the effects of freeze drying on the encapsulation, solubility, and re-dispersibility of protein–hydrophobic active substance nanoparticles remain unclear. Modulating the protein–hydrophobic active substance–water triad interactions is essential to minimize activity loss and aggregation during dehydration/rehydration.

Ultrasound is a promising means of functionally modifying proteins; a consensus exists that its effects of cavitation, heating, dynamic agitation, shear, and turbulence could modify the physicochemical, functional, and structural aspects of proteins [27,45], thus improving their overall functional properties, such as solubility, emulsification, and foaming [9,15,58]. Ultrasound was also found to induce protein structure unfolding, increase the hydrophobicity of protein surface, reduce protein particle size [22,29], change the binding mode of protein and hydrophobic active substance, and facilitate the encapsulation of active substances [16,38,54]. Besides, changes in molecular unfolding, dispersibility, molecular flexibility, and hydrophobic–hydrophilic balance induced by moderate ultrasound may lead to more stable proteins and increased resistance [67]. Ultrasound may become a convenient and efficient means to modulate the protein–hydrophobic active substance assembly system during freeze drying. However, excessive ultrasound could further expose protein hydrophobic groups and increase random coil, forming unstable small protein molecules. These molecules recombine under hydrophobic interactions to form larger aggregates [15,51], which may adversely affect the freeze drying of protein nanocomplexes.

At present, limited information could be found on the changes in protein–polyphenol nanocomplexes during freeze drying, and reports on the regulatory effect of ultrasound on the protein and polyphenol coexistence system in freeze drying are lacking. Therefore, in the present study, an egg-white protein isolate–curcumin (*EPI*–Cur) nanocomplex was used as a model to investigate the mechanism of the effect of freeze drying on protein–polyphenols nanocomplexes' aggregation degree. This study modulated the interaction between *EPI* and curcumin by controlling ultrasound time to regulate the degree of aggregation of the complexes during lyophilization and to improve the re-dispersibility of the complexes and the loading of curcumin. The results could provide a theoretical basis for the changes and regulatory mechanisms of the protein–hydrophobic polyphenol assembly system in freeze drying and provide new ideas for the development of lyophilized powder with easily soluble curcumin.

2. Materials and methods

2.1. Test Materials

EPI was obtained from Jinhai Food Industry Co., Ltd. (Qinhuangdao, China). Curcumin was purchased from Sigma–Aldrich Corp (St. Louis, MO, USA). Concentrated hydrochloric acid, sodium hydroxide, and phosphate were provided by Nanjing Chemical Reagent Equipment Co., Ltd., China. 8-Aniline-1-naphthalene (ANS) was purchased from Shanghai Aladdin Biochemical Technology Co., Ltd. (Shanghai, China). All chemicals and reagents used were of at least analytical grade.

2.2. Preparation of EPI–Cur complexes under different ultrasound times

2.2.1. Ultrasound treatment

EPI was fully dissolved in ultra-pure water and stirred overnight at 4 °C using a magnetic stirrer to fully dissolve. Then, a Vibra-Cell TM ultrasonic processor (VC 750, Sonics & Materials, Inc., USA) fitted with a 6 mm-diameter probe (630–6435, Sonics & Materials, Inc., USA) was used to treat *EPI* suspension. The *EPI* samples were subjected to ultrasound treatment (frequency of 20 kHz and power of 400 W) for 0, 6, 12, 18, and 24 min (with pulse mode duration of 2 s on and 2 s off). The untreated sample was used as a control and stored at 4 °C. The probe was immersed in the *EPI* suspension to a depth of 1 cm during ultrasound treatment. The sample remained in an ice bath, and the temperature was kept below 8 °C.

2.2.2. Preparation of EPI–Cur complex

In accordance with the team's previously reported method [62], the *EPI* treated with different sonication times was placed on a magnetic stirrer and kept rotating at a high speed of 600 rpm. The pH of the solution was adjusted to 12.0 by slowly adding NaOH (4 mol/L), during which it was stirred at a constant speed for complete reaction. After 30 min of incubation, the appropriate amount of curcumin was added to the protein solution so that the concentration of curcumin in the solution was 0.2 mg/ml. After allowing the curcumin and *EPI* to fully react for 30 min in the dark, the pH of the solution was adjusted to 7.0 with HCl (4 mol/L). After the addition of curcumin, the solution was incubated away from light and the *EPI*-Cur solution was stored away from light in cold storage at 4 °C. All procedures conducted in the control group were the same, except for curcumin encapsulation.

2.3. Characteristics of EPI–Cur complexes after ultrasound treatment

2.3.1. Dynamic light scattering (DLS)

The particle size of the samples was determined using DLS techniques. The *EPI*–Cur complex dispersion and *EPI* solution were diluted 10 times with PBS (20 mM, pH 7.0) and then added to the sample tank. The particle size was measured by Zetasizer Nano-ZS 90 instrument (Malvern Instruments, Worcestershire, UK) equipped with a 4 Mw He-Neon laser. The wavelength output at 24 °C was 633 nm, and the monitoring angle was set to 90°.

2.3.2. Turbidity

The turbidity of each group of samples was measured in accordance with Wu et al [62]. The absorbance of the compound solution at 600 nm was determined by a multifunction enzyme labeling instrument (Spectra Max M2, Molecular Devices Limited, San Francisco, California, USA), and all the measurements were repeated more than three times.

2.3.3. EPI solubility

The solubility of *EPI* was determined is as follows: in accordance with the official instructions, the protein concentration of different treatment groups was determined using the Pierce BCA Protein Assay Kit (Thermo Fisher Scientific, USA), and then the undissolved part was removed by centrifugation at 10,000 g for 10 min. Next, the protein content was determined using the BCA Kit. The ratio of the two is referred to as protein solubility.

2.3.4. Ee

The EE of the complexes was slightly modified using a previous method [59]. All prepared complex dispersions were centrifuged at 10,000 g for 10 min to remove insoluble particles in the solution. The supernatant was then diluted 40 times with absolute ethanol and allowed to stand for 20 min at room temperature in the dark. The upper organic phase was taken, and its absorbance at 425 nm was measured with a microplate reader. Then, the curcumin concentration was calculated in accordance with the standard curve of Cur–ethanol solution ($R^2 = 0.999$).

$$EE\ (\%) = \frac{curcumin\ concentration\ in\ supernatant}{The\ total\ concentration\ of\ curcumin\ in\ compound\ solution} \times\ 100\ \% \quad (1)$$

2.4. Structure and stability of EPI–Cur complexes

2.4.1. h_0

The H_0 of *EPI* and the *EPI*–Cur complex was determined using a previous method, with modifications [59]. In brief, 20 μL of ANS (20 mM in 20 mM PBS, pH 7.0) was added to a 4 mL sample. After 20 min of reaction at room temperature (approximately 25 °C), the fluorescence spectra of the samples were measured by a microplate reader (Spectra Max M2, Molecular Devices Limited, San Francisco, California, USA). The excitation wavelength was 380 nm, and the emission wavelength range was 430–570 nm. All procedures used in the control group were the same, except for curcumin encapsulation.

2.4.2. UV-vis spectroscopy

The *EPI*–Cur complexes were diluted fivefold with PBS (20 mM, pH 7.0). By using the above multifunction microplate reader, with PBS (20 mM, pH 7.0) as blank, the absorption spectra of the complexes were scanned in the range of 300–600 nm.

2.4.3. Fluorescence spectroscopy

The fluorescence spectra of the samples were measured by a microplate reader (Varioskan Flash, Thermo Scientific Company, Waltham, MA) at room temperature (25 °C). All the above samples were diluted 10-fold with PBS (20 mM, pH 7.0) by using the method of Wu et al. [59], with appropriate modifications. The emission spectrum was scanned from 300 nm to 500 nm at an excitation wavelength of 280 nm.

2.4.4. Determination of physical stability

The physical stability of the *EPI*–Cur complex was characterized by multiple light scattering and storage stability.

Multiple light scattering was monitored by scanning a series of backscattered light from the bottom to the top of the sample with the use of a Turbiscan multiple light scattering analyzer (Turbiscan Tower, Formulation, Toulouse, France). In particular, 25 mL of the emulsion was transferred into a cylindrical sample bottle and scanned at 24 °C for 3 h. Then, the optical properties of each group of samples were recorded. The Turbiscan stability index (TSI) could characterize unstable phenomena, such as coalescence, flocculation, and emulsification; it is obtained by calculating data changes in the backscattered light intensity at different positions of the sample unit. The smaller the TSI value is, the better the stability of the sample.

For determination of storage stability, a freshly prepared *EPI*–Cur solution was immediately transferred to a 20 mL-transparent glass bottle, and sample changes after 0 and 10 days of storage at 25 °C were observed.

2.5. Freeze drying

Freeze drying is currently the most widely used and effective method to prepare stable solid protein-based drugs. In accordance with the research results in the previous chapters, the *EPI*–Cur composite solution sonicated for 0, 12, and 24 min was selected and placed into a freeze dryer (Alpha 2–4 LSC plus, Marin CHRIST, Osterode, Germany) for freeze drying. The drying time was 48 h, and the temperature was −80 °C.

2.6. Characterization of EPI–Cur freeze-dried powder

2.6.1. X-ray diffraction (XRD) analysis

The XRD patterns of *EPI*, curcumin, and freeze-dried powder prepared under different ultrasound conditions (0, 12, 24 and min) were analyzed by a Bruker D8 diffractometer (Bruker, Karlsruhe, Germany). The measurement conditions were as follows: voltage of 40 kV, current of 40 mA, scanning speed of 2°/min, $2\theta = 5–55°$, and X-ray light source of Cu-Ka ($\lambda = 0.15418$ nm).

2.6.2. Particle morphology of the powder

The particle morphology of the powder was observed by scanning electron microscopy (ZEISS HD, Oberkochen, Germany). The freeze-dried samples of each group were ground into powder, and the appropriate amount of freeze-dried powder was placed on the conductive gel of the sample table respectively, and dispersed into a thin layer. The floating powder was blown off with an ear ball, and gold was sprayed into the sample cavity of the electron microscope for scanning observation. The acceleration voltage was 10 kV.

2.6.3. Asymmetrical flow field-flow fractionation (AF4)

AF4 is one of the separation methods in flow field separation. Its separation conditions are mild and do not destroy the original structure and morphology of the sample. They could also be analyzed online by various detectors, such as UV–vis detector, fluorescence detector, differential refractive index (Dri) detector, multi-angle light scattering (MALS), and DLS, to obtain more detailed information about the sample. In this study, the *EPI*–Cur complexes were separated and characterized by connecting AF4 to a series of three detectors: UV, MALS, and Dri.

The AF4 system used in this study is the Eclipse 2 separation system (Wyatt Technology Europe, Dernbach, Germany). It was connected to a 500 th UV–vis detector (Chrom Tech Inc., MN, USA) operating at 280 nm, a MALS detector (Wyatt Technologies, Santa Barbara, CA) at 690 nm, and a 1260 Dri (Agilent Technologies, Waldbronn, Germany). The Agilent 1100 pump with an online vacuum degasser (Agilent Technologies, Waldbronn, Germany) delivered the carrier liquid to the AF4 channel. The injection concentration was maintained at 1.0 mg/mL. The injection volume was 20 μL, and the carrier solution was 20 mM PBS buffer (pH 7.0). Data were processed by Peakfit version 4, Sigmaplot 12.3, and other software.

2.6.4. Retention rate and loading of curcumin

After 10 mg of lyophilized powder was reconstituted with 2 mL of deionized water, it was centrifuged at 10,000 g for 10 min to remove insoluble curcumin crystals, and the concentration of curcumin was

calculated in accordance with the method in 2.3.4. The concentration of curcumin in the supernatant refers to the concentration of curcumin in the freeze-dried powder.

The retention rate of curcumin (RC) refers to the percentage of curcumin concentration in the freeze-dried powder and the concentration of curcumin in the compound before freeze drying.

The load of curcumin (LC) refers to the ratio of the content of curcumin in the freeze-dried powder to the quality of the *EPI* powder.

$$RC\ (\%) = \frac{Concentration\ of\ curcumin\ in\ freeze-dried\ powder}{Concentration\ of\ curcumin\ in\ complex} \times 100\ \% \quad (2)$$

$$LC\ (mg/g) = \frac{amount\ of\ curcumin\ encapsulated}{amount\ of\ EPI\ powder} \quad (3)$$

2.6.5. Solubility and re-dispersibility of the powder

The solubility of the dried powder was analyzed by spectrophotometry and adjusted slightly in accordance with Chen et al [6]. Deionized water (3 mL) was placed in a colorimetric plate (3 mL, 1×1 cm cross-section), and then 15 mg of lyophilized powder was added separately into a spectrophotometer (EU-2600R, SHANGHAI ONLAB, China). A timer was then started to record the change in the absorption value of the sample at 425 nm at regular intervals until the absorption value reached its maximum without further change. The slope of the absorption value at the beginning of dispersibility and the maximum absorption value indicated the sample's dispersibility rate and capacity, respectively.

A positive fluorescence microscope was used to observe the re-dispersible state of the *EPI*–Cur freeze-dried powder (Scope.A1, Carl Zeiss, Germany). An appropriate amount of freeze-dried *EPI*–Cur powders under different treatments was fully dissolved in deionized water separately and then placed in 80 μL solution onto the slide glass. The samples were covered with a cover glass to ensure no air bubbles were present between the glasses. The microstructure of the solution was observed, and images were taken with a 20-fold objective lens. At least five images were randomly taken from each group of samples.

2.7. Statistical analysis

All experiments were divided into three batches, each batch of *EPI* was repeated three times in different treatment groups, and each group was analyzed three times. In order to avoid the error of the instruments, each analysis replicate was repeated three times, and the results were reported as averages and standard deviations. Statistical analysis was performed using SAS 8.0 software with one-way ANOVA and Duncan's multiple range tests (SAS Institute Inc., Cary, NC, USA). A p-value of $\leq$ 0.05 was considered statistically significant.

3. Results and discussion

3.1. Properties of EPI–Cur complexes

3.1.1. Particle size of the complexes

The heating, stirring, cavitation, and turbulence capabilities of ultrasound have been proven to cause changes in the physicochemical, function, and even structure of proteins [21]. Table 1 shows the change in the particle size of *EPI* and the *EPI*–Cur complexes with ultrasound time. The *EPI* that did not undergo ultrasound was found to have the largest z-average diameter of 345 nm, explaining the higher turbidity values obtained under this treatment. With the prolongation of ultrasound time, the particle size of *EPI* decreased first and then grew as the ultrasound time increased. At 12 min, *EPI* had the smallest particle size (Z-average particle size of 182 nm), and the particle size of *EPI*–Cur nanocomplex was further reduced (Z-average particle size of 169 nm). This finding demonstrated that moderate mechanical effects, such as cavitation and turbulence, caused by ultrasound could disintegrate natural protein aggregates and make them disperse into smaller protein particles, thus reducing particle size and enhancing protein dispersibility. The particle size rapidly grew with increasing ultrasound duration (after 12 min) due to the exposure of an increasing number of hydrophobic sites and the development of new aggregates in a continuous collision. The particle size of *EPI* decreased after combining it with curcumin, consistent with the result of Wang et al. [59], indicating that the interaction between curcumin and protein generated a more compact structure.

Table 1
Effect of ultrasonic time on protein solubility, encapsulation efficiency, particle size and turbidity of *EPI* and *EPI*-Cur.

Ultrasound time (min)	Particle size (nm)		Turbidity ($\times 10^{-2}$)		Protein Solubility (%)	EE (%)
	EPI	*EPI*-Cur	*EPI*	*EPI*-Cur	*EPI*	*EPI*-Cur
0	345.10 ± 8.94^{Aa}	286.67 ± 6.88^{Ba}	22.3 ± 1.65^{Aa}	12.24 ± 1.08^{Ba}	86.71 ± 1.49^{d}	71.64 ± 0.64^{d}
6	228.33 ± 7.09^{Ab}	208.47 ± 5.67^{Bb}	14.89 ± 0.35^{Ab}	9.47 ± 0.26^{Bb}	89.69 ± 0.34^{c}	70.12 ± 2.01^{d}
12	182.17 ± 2.85^{Ad}	169.53 ± 6.93^{Bc}	13.39 ± 0.20^{Ad}	9.06 ± 0.07^{Bb}	95.11 ± 0.26^{a}	87.37 ± 0.48^{a}
18	204.63 ± 3.70^{Ac}	166.83 ± 2.24^{Bc}	13.81 ± 0.27^{Ac}	8.71 ± 0.17^{Bb}	93.13 ± 1.03^{b}	80.77 ± 2.23^{b}
24	210.50 ± 6.14^{Ac}	176.23 ± 7.71^{Bc}	14.18 ± 0.20^{Ac}	8.99 ± 0.14^{Bb}	88.13 ± 0.81^{c}	77.41 ± 0.95^{c}

Data are presented as the mean ± standard deviation (SD) from triplicates. Different letters a-d indicate significant differences within rows ($p < 0.05$). The letters A and B represent significant differences within columns ($p < 0.05$).

3.1.2. Turbidity

Turbidity refers to the degree to which a solution obstructs the passage of light; it could accurately reflect the degree of protein aggregation [30]. As shown in Table 1, the turbidity of the *EPI* samples decreased in the sequence 0 min > 6 min > 18 min > 24 min ≈ 12 min following various treatment times, consistent with the particle size distribution of *EPI*, because the magnitude of the protein aggregation is negatively correlated with particle size and turbidity. The *EPI*'s particle size and turbidity decreased significantly after 12 min, demonstrating that mild ultrasound could increase the dispersibility and provide favorable conditions for the assembly of curcumin.

3.1.3. Protein solubility

Protein solubility is essential for the encapsulation of curcumin, and protein properties could be enhanced by increasing protein solubility to improve the encapsulation of active substances [25,61]. Table 1 illustrates the influence of various ultrasound times on the solubility of *EPI* in the present study. Protein solubility increased initially and gradually dropped with increasing ultrasound time, with *EPI* solubility reaching a maximum after 12 min. Other proteins, such as soy protein isolate [42], myofibrillar protein [2], exhibit comparable tendencies. The mechanical effect of moderate ultrasound disrupted the aggregation of natural proteins, and the moderate unfolding of the protein structure increased the contact of proteins with water, thus improving their solubility. The structural unfolding of the proteins contributed to the exposure of hydrophobic groups, thus providing more binding sites for curcumin, and the decrease in particle size and turbidity demonstrated the role of ultrasound in improving protein dispersion.

3.1.4. Ee

As shown in Table 1, the EE of the *EPI*–Cur complex in 12 min of ultrasound significantly improved ($p < 0.05$), indicating that moderate ultrasound could effectively promote curcumin entrapment in *EPI* and form a stable composite solution. When the ultrasound times were 12 and 18 min, the EE of the complex solution could reach around 80 %, demonstrating that most of the curcumin in the solution could effectively bind to *EPI*. The EE under 6 min of treatment was not significantly different from the untreated group, probably due to insufficient sonication time resulting in lower protein dispersion and insufficient exposure of the hydrophobic region, which was confirmed by the results of surface hydrophobicity studies. Chen et al. [9] also discovered that ultrasound helps polyphenols, such as EGCG, bind to proteins.

3.2. Structure and stability of the complexes

3.2.1. Surface hydrophobicity (H_0)

As a fluorescent probe, ANS preferentially binds to hydrophobic sites, and it is widely used to understand the number and distribution of hydrophobic plaques on the sample surface [57]. As shown in Fig. 1, after ultrasound was applied for 12 min, the H_0 of the *EPI* reached its maximum. The mechanical interaction during ultrasound exposed more hydrophobic regions of proteins and increased the sample H_0. In addition, the *EPI* provided more binding sites for curcumin, indicating that more curcumin could bind through hydrophobic interaction. This finding is consistent with the EE results. When combined with curcumin, the hydrophobic interaction between the aromatic ring with the hydroxyl group in the curcumin structure and the hydrophobic region of the protein surface resulted in a significantly decreased H_0 [69].

3.2.2. UV-vis spectroscopy

As shown in Fig. 2, UV-vis spectroscopy was used to determine the effect of different ultrasound times (0, 6, 12, 18, and 24 min) on the *EPI*–Cur composite solution. In general, the intensity of the maximum absorption peak in the absorption spectrum could reflect the interaction between proteins and small molecules. An absorption peak of 425 nm was applied to characterize the interaction between curcumin and protein. The results showed that with the increase in ultrasound time, the maximum absorption peak increased first and then decreased. The UV absorption peak of the composite solution was the highest under 12 min, when the binding effect of curcumin with protein was the strongest, and the concentration of curcumin in the solution was the highest, which was confirmed by the results of EE in Table 1. The maximum

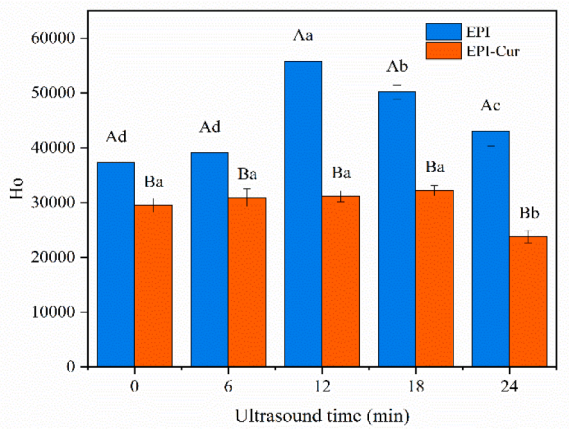

Fig. 1. Surface hydrophobicity of *EPI* and *EPI*-Cur under different ultrasonic times. (Error bars are standard deviations of triplicates. Different letters a-c indicate significant differences between different ultrasound time treatments ($p < 0.05$). Letters A and B represent significant differences between *EPI* and *EPI*-Cur within the same ultrasound time ($p < 0.05$)).

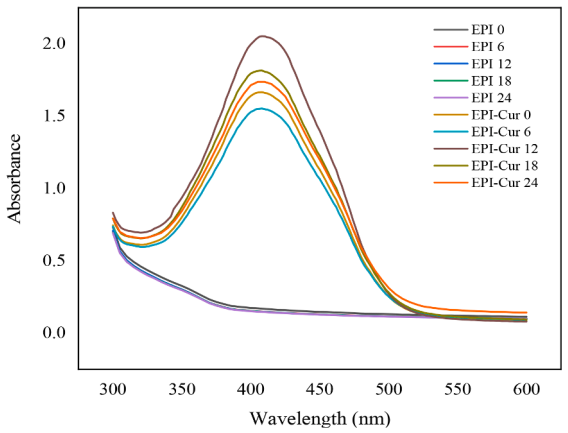

Fig. 2. UV–vis spectra of *EPI*-Cur complex at the different ultrasonic times. (0, 6, 12, 18, and 24 represent the ultrasound time in minutes).

absorbance of the untreated *EPI*–Cur complex was significantly lower than that of the 12, 18, and 24 min-treated groups ($p < 0.05$), indicating that ultrasound treatment could enhance the interaction between curcumin and *EPI*. By contrast, the maximum absorption intensity decreased to some extent after 12 min, possibly due to the hydrophobic aggregation of *EPI* or the destruction of the curcumin binding site caused by excessive ultrasound, resulting in decreased curcumin binding.

3.2.3. Fluorescence spectroscopy

Under different ultrasound treatments, the changes in the tertiary structure of *EPI* and the *EPI*–Cur complex were mainly determined by endogenous fluorescence spectra, as shown in Fig. 3. No apparent red shift or blue shift was found in the peak position of the endogenous fluorescence spectrum of the treated *EPI*. In addition, the *EPI* had diverse fluorescence intensities under different ultrasound treatments (0,6, 12, 18, and 24 min). The fluorescence intensity increased gradually with the increase in ultrasound time and reached the maximum at 18 min. This phenomenon indicated the process of dispersion and re-aggregation of *EPI* under the action of ultrasound. The results showed that the proteins had different structural characteristics under different ultrasound treatment times. Therefore, *EPI* with different structures may have distinct entrapment effects when binding with curcumin. After such binding, the fluorescence intensity of the complex was significantly lower than that of the *EPI* due to the fluorescence quenching effect of curcumin. This effect may reflect the entrapment effect of curcumin.

3.2.4. Physical stability

Fig. 4A shows the *EPI*–Cur complexes stored in the dark for 1 and 10

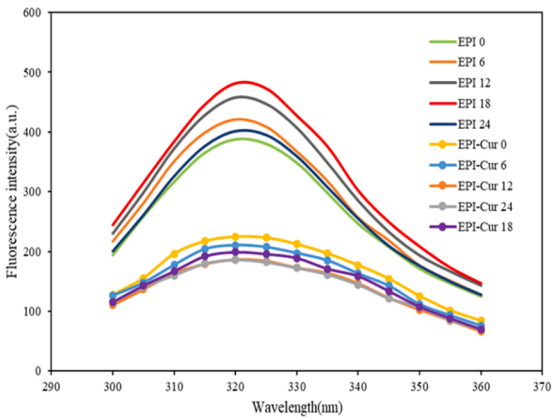

Fig. 3. Fluorescence spectra of *EPI* and *EPI*-Cur at different ultrasonic times. (0, 6, 12, 18, and 24 represent the ultrasound time in minutes).

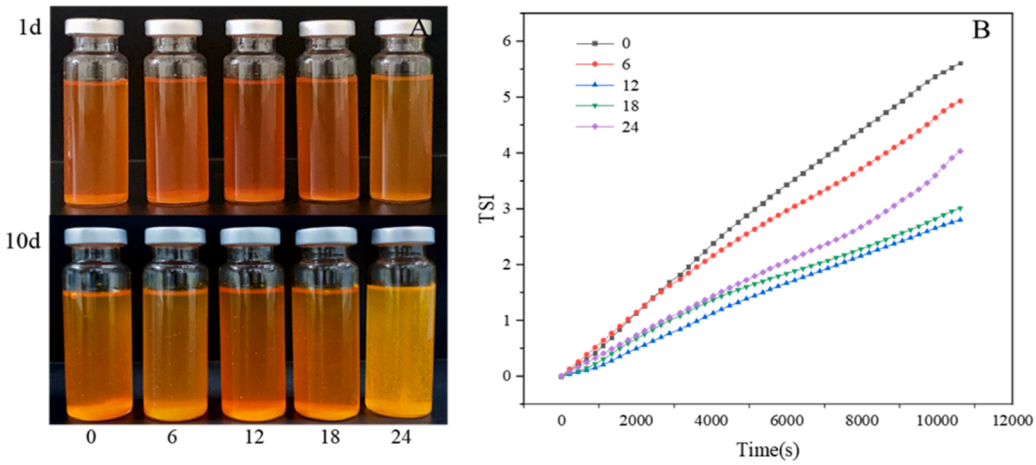

Fig. 4. The visual appearance of *EPI*-Cur complex solution at 25 °C for 1, 10 d (A); TSI of *EPI*-Cur complexes at different ultrasound times as a function of time (temperature maintained at 24 ℃) (B).

days at room temperature (25 °C) with varying ultrasound times. The *EPI*–Cur complex showed distinct colors under different ultrasound times because ultrasound changed the EE of curcumin. The 12 min-treated group had the highest EE and therefore the darkest color of the solution. After 10 days of storage, the 24 min-treated group exhibited a considerable amount of particle precipitation because excessive ultrasound disrupted the hydrophobic–hydrophilic balance between proteins, thus speeding up the collision, aggregation, and precipitation of complex particles. After 10 days of storage, the *EPI*–Cur complex in the 12 min-treated group were least aggregated compared with the other groups. Therefore, 12 min of ultrasound improved the stability of the composite particles.

TSI was employed to compare their stability more thoroughly. The TSI value could be used to determine the dynamic instability of an emulsion by combining changes in instability (such as emulsification, flocculation, and coalescence). The greater the TSI value is, the more unstable the system [13]. The TSI values of all samples increased with the extension of storage time, as shown in Fig. 4B, suggesting that the solution was in a dynamically unstable state. Overall, the complex without ultrasound treatment had the highest TSI (5.61), followed by the 6 min-treated group (4.93), whereas the 12 min-treated group had the lowest (2.80). After 8000 s, the slope of the TSI curve in the 24 min-treated group suddenly increased, and it was significantly higher than that in the other groups. This finding showed that excessive ultrasound caused a sharp decline in the sample stability after long-term storage, consistent with Fig. 4A.

3.3. Characterization of EPI–Cur lyophilized powders

3.3.1. XRD analysis

As shown in Fig. 5, curcumin had characteristic peaks at 9.05°, 17.48°, etc., indicating that it was highly crystalline, and these characteristic peaks were consistent with previous reports [19,41]. Meanwhile, *EPI* had no prominent sharp peaks, only two amorphous peaks at 8.98° and 19.96°. In the three *EPI*–Cur complexes formed by freeze drying, the classic curcumin peaks almost totally disappeared, the peak at 31.80° strengthened, and a new peak developed at 45.51°, indicating a potential crystal change during the assembly and freeze-drying process. The crystallinity of curcumin was calculated by Jade software. The crystallinities of curcumin, *EPI*, the untreated group, the 12 min-treated group, and the 24 min-treated group were 85 %, 4 %, 30 %, 6 %, and 17 %, respectively. The compound's crystallinity was dependent on the presence and position of curcumin. Curcumin could be more effectively incorporated into *EPI* when treated for 12 min, and the curcumin in the complex existed in an amorphous form. The crystallinity of the 24 min-treated group was significantly higher than that of the 12 min-treated group, indicating that curcumin leaked and formed new crystals during freeze drying. This phenomenon could be attributed to the further exposure of protein hydrophobic groups by excessive ultrasound, which made the structure become unstable. In addition, the expansion and denaturation were intensified under low-temperature stress and concentration effect during freeze drying, resulting in curcumin leakage.

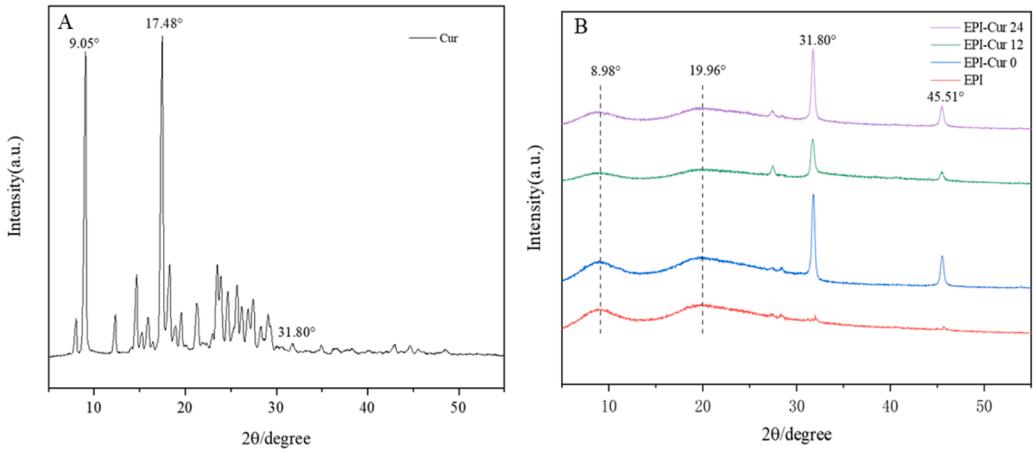

Fig. 5. XRD patterns of curcumin(A), *EPI*, and the freeze-dried curcumin-loaded nanoparticles (B).

3.3.2. Particle morphology of the lyophilized powder

The particles morphology of the three freeze-dried powders was observed by SEM, and the result is shown in Fig. 6. The microstructure of the freeze-dried *EPI*–Cur powder treated under different ultrasound conditions obviously changed compared with that of the untreated group. The untreated *EPI*–Cur lyophilized powder was flaky, with more regularly shaped attachments on its surface (Fig. 6A1), which were probably crystals of free curcumin. Most of its particles had smooth surfaces and varied shapes and sizes; the particles appeared to be clearly aggregated, and the aggregates were large and irregularly shaped, with small spaces between them (Fig. 6A2). The 12 min-treated group had a smooth surface, small particle size, and uniform distribution. No apparent bulk aggregation was found (Fig. 6B). The 24 min-treated group was rough and uneven, and the aggregate was the maximum aggregation (Fig. 6C). A notable detail that in the 0 and 24 min-treated groups, many aggregates were formed by small particles surrounding many larger ones, which combined to form larger aggregates. On the contrary, no such phenomenon was found in the 12 min-treated group. The composite solution had the highest EE when treated for 12 min, indicating that the hydrophobic regions of the protein were occupied by curcumin, thus reducing the hydrophobic aggregation caused by exposure of the hydrophobic regions. In addition, moderate ultrasound increased the flexibility of the protein [52,63], leading to its increased resistance to freeze drying. The low encapsulation rate of curcumin in the untreated group resulted in a large number of small molecules of free curcumin in the complex. Studies have shown that free curcumin could aggregate with one another by hydrophobic interactions and subsequently form further clusters by hydrogen bonding, and curcumin clusters may bridge protein chains through hydrophobic and hydrogen bonding interactions, inducing protein–protein residues near the binding site to come furtherly closer, thus allowing proteins to intertwine with one another and form aggregates with larger size [65,66]. During excessive ultrasound, the hydrophobic regions of the proteins were overexposed, and proteins formed unstable soluble aggregates under hydrophobic interactions, thereby exacerbating the aggregation during freeze drying.

3.3.3. AF4

AF4 is a mild and rapid size-based separation method where components with smaller hydration diameters are eluted first [18]. The UV signal intensity showed the three tested samples' aggregation degree and gyration radius (Rg) distributions. The AF4UV/Vis fractal images of *EPI*–Cur complexes under different ultrasound times are shown in Fig. 7. As the ultrasound time was increased from 0 min to 24 min, the signal intensity of small protein particles (which peaked at approximately 0.8 min) gradually increased. However, the signal intensity during 12 and 24 min of treatments decreased significantly in the large protein particles, with that of the 12 min-treated group being the lowest. The results showed that the aggregation degree and Rg size of the sample was in the order 0 > 24 > 12 min, and longer ultrasound time was more favorable to forming small *EPI*–Cur complex. The destruction of large aggregates by ultrasound also had a significant effect after freeze drying. The degree of curcumin-mediated hydrophobic aggregation of proteins was related to the free curcumin content, and more free curcumin formed larger aggregates; thus, the highest aggregation was observed in the untreated group. The relative increase in the aggregation degree of the 24 min-treated group was probably due to excessive energy input, which further disrupted the protein structure, making the system more unstable and prone to new aggregation in lyophilization.

3.3.4. Retention rate and loading of curcumin

The retention rate and loading of freeze-dried curcumin powder prepared under different ultrasound treatments (0, 12, and 24 min) are shown in Fig. 8. After ultrasound treatment of 12 min was conducted,

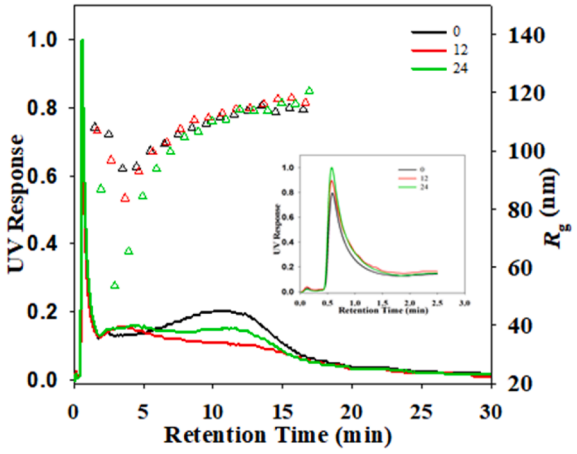

Fig. 7. AF4-UV fractograms (lines) and Rg distributions of *EPI*-Cur lyophilized after 0, 12, and 24 min pre-ultrasound treatment.

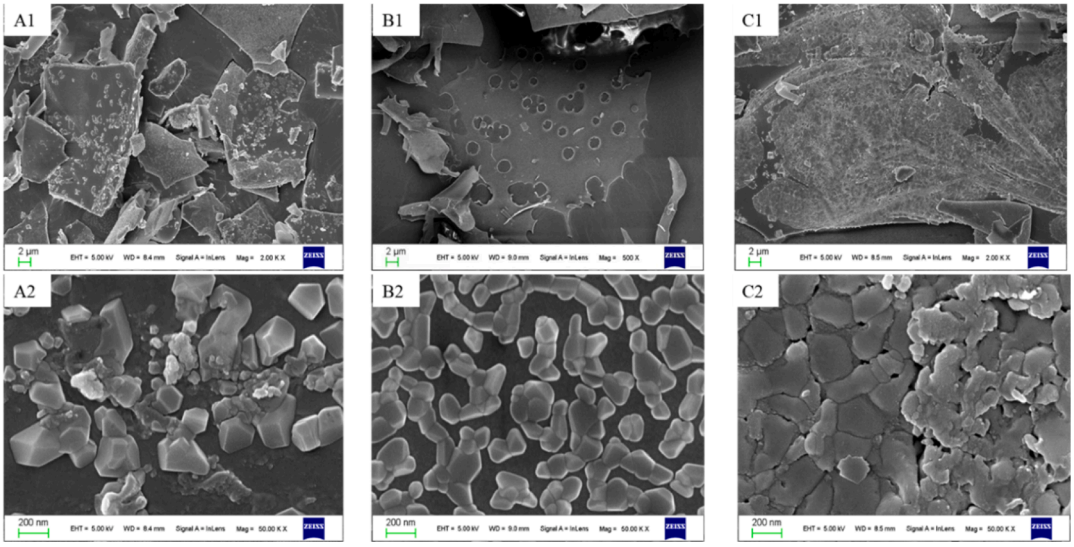

Fig. 6. Electron microscopic scanning images of the three *EPI*-Cur complexes prepared by freeze-drying (A: control group; B: 12 min treatment group; C: 24 min treatment group; 1–2: 2 μm and 200 nm scale bar).

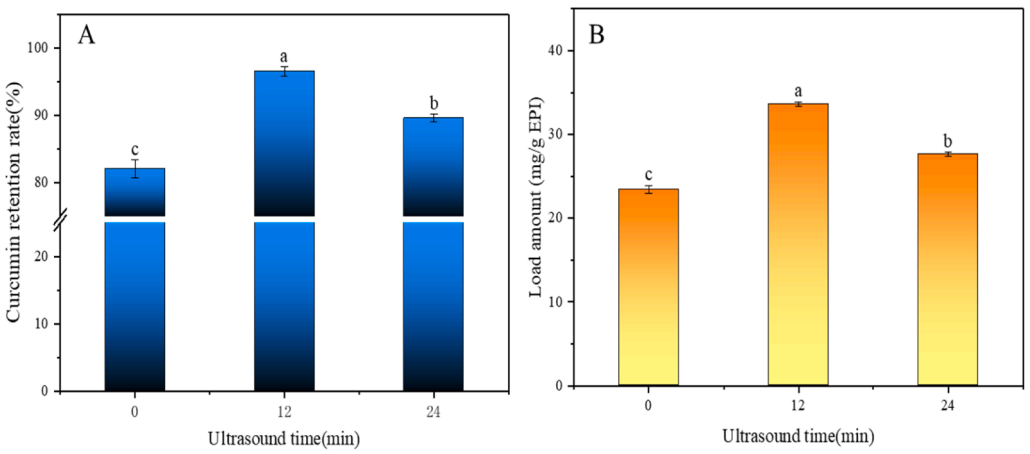

Fig. 8. The retention rate and loading of Curcumin freeze-dried powder were prepared after different pre-ultrasonic treatments (0, 12, 24 min). (Error bars are standard deviations of triplicates. Statistical differences were presented by dissimilar letters in the same graph among the samples ($p < 0.05$)).

the retention rate of the freeze-dried *EPI*–Cur powder increased from 82.06 % to 96.54 %, and the load increased from 23.42 mg/g *EPI* to 33.60 mg/g *EPI*. Meanwhile, the retention rate of curcumin in the untreated sample was 82.06 %, indicating that approximately 18 % of curcumin molecules were decomposed or exfoliated during freeze drying. This decrease may be attributed to the excessive aggregation, denaturation, or inactivation of protein carriers, directly or indirectly caused by low-temperature stress and drying stress during freeze drying. Besides, the untreated *EPI* had a larger particle size and poor dispersion, and more free curcumin in the solution could further cause protein aggregation, thus affecting the activity and curcumin loading capacity of the embedding material.

3.3.5. *Solubility and re-dispersibility of the powder*

Solubility and re-dispersibility are the most critical factors affecting powder products' quality and consumer acceptability. With the prolongation of time, the solubility of the powder and the concentration of curcumin increased, causing the absorbance at 425 nm to increase. Thus, the solubility of the powder sample could be obtained indirectly by analyzing the change in absorbance at 425 nm. As shown in Fig. 9A, the absorption value as the vertical coordinate and the time as the horizontal coordinate for the graph could reflect the dispersibility process of the powder. In the initial stage of dispersibility (0–3 min), the absorbance of the solution increased sharply and then tended to be in equilibrium. The absorption slope (Ko) of the freeze-dried curcumin powder prepared by ultrasound (12 and 24 min) was significantly higher than that of the untreated group at the beginning, and the final solution equilibrium absorbance was higher. This finding showed that ultrasound could improve the rate of dispersibility and solubility of the freeze-dried *EPI*–Cur powder.

Fig. 9B and C show the appearance of the solution of the lyophilized powder after re-dissolution and the microstructure of the heavy

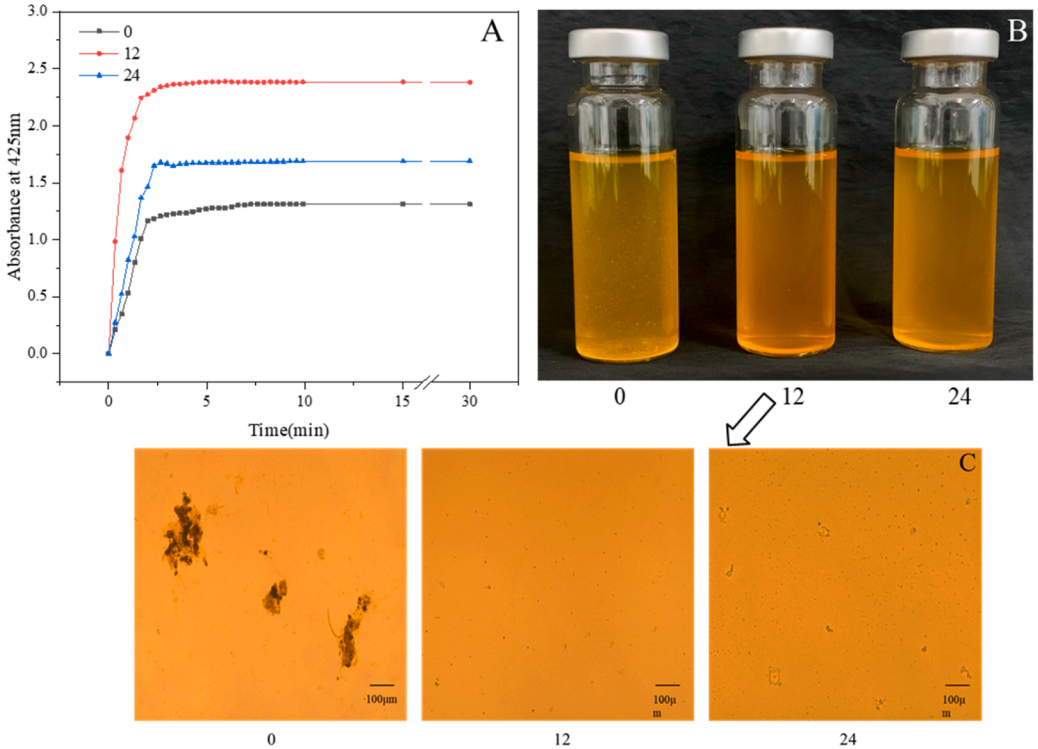

Fig. 9. Curcumin retention rate (A), loading amount (B), fluorescence upright microscope (C) of three groups of *EPI*-Cur powders after reconstitution (0, 12, 24 min).

dispersion observed under the microscope, respectively. Large curcumin aggregates could be seen in the naked eye in the untreated complex solution. Noticeable particles were also observed under the microscope. The curcumin in these aggregates could not be dissolved in the solution, which is one of the reasons for the low retention of curcumin in the freeze-dried powder.

4. Conclusion

This study clarified the mechanism by which ultrasound treatment regulates *EPI*–Cur assembly and its effect on freeze drying and re-dispersibility. The results indicated that ultrasound treatment significantly affected the entrapment effect and complex stability of curcumin via altering the physical properties and tertiary protein structures. Ultrasound treatment also reduced the particle size of *EPI* and facilitated protein structural expansion, thus increasing the number of binding sites for curcumin. Excessive energy input resulted in hydrophobic aggregation of the system, which was detrimental to curcumin entrapment and composite solution storage. The free curcumin in the system generated curcumin clumps throughout the freeze-drying process, resulting in protein bridging and aggregation due to hydrophobicity and hydrogen bonding, thus impairing the re-solubility of freeze-dried products. The freeze-dried products from the 12 min-treated group had the best re-dispersibility and the lowest crystallinity, with a curcumin load of up to 33.60 mg/g *EPI*, indicating that the *EPI*–Cur complex could withstand various adverse effects during the freeze-drying process. Such ability may be attributed to the change in the *EPI* structure, which alters the spatial position of curcumin binding and prevents leakage and aggregation. In this study, the structure of *EPI* and its interaction with curcumin were regulated by ultrasound to explore the dynamic concentration mechanism and dispersion of *EPI*–Cur nanocomposites in the freeze-drying and re-dispersibility processes, providing theoretical value for the delivery of hydrophobic active substances.

Declaration of Competing Interest

The authors declare that they have no known competing financial interests or personal relationships that could have appeared to influence the work reported in this paper.

Data availability

The data that has been used is confidential.

Acknowledgements

This research was funded by National Key R&D Program of China (2021YFD2100503), National Natural Science Foundation (32172243) and China Agriculture Research System (CARS-41).

References

[1] M. Abdollahi, J. Axelsson, N. Carlsson, G.M. Nylund, E. Albers, I. Undeland, Effect of stabilization method and freeze/thaw-aided precipitation on structural and functional properties of proteins recovered from brown seaweed (Saccharina latissima), Food Hydrocolloids 96 (2019) 140–150, https://doi.org/10.1016/j.foodhyd.2019.05.007.

[2] A. Amiri, P. Sharifian, N. Soltanizadeh, Application of ultrasound treatment for improving the physicochemical, functional and rheological properties of myofibrillar proteins, International Journal of Biological Macromolecules 111 (2018) 139–147.

[3] Anandharamakrishnan, C. (2014). Nanoencapsulation of Food Bioactive Compounds. In C. Anandharamakrishnan (Ed.), *Techniques for Nanoencapsulation of Food Ingredients*(pp. 1-6). Springer New York.

[4] J.A.M. Berghout, P. Venema, R.M. Boom, A.J. van der Goot, Comparing functional properties of concentrated protein isolates with freeze-dried protein isolates from lupin seeds, Food Hydrocolloids 51 (2015) 346–354.

[5] E.H. Cao, Y.H. Chen, Z.F. Cui, P.R. Foster, Effect of freezing and thawing rates on denaturation of proteins in aqueous solutions, Biotechnology and Bioengineering 82 (6) (2003) 684–690, https://doi.org/10.1002/bit.10612.

[6] F.-P. Chen, L.-L. Liu, C.-H. Tang, Spray-drying microencapsulation of curcumin nanocomplexes with soy protein isolate: Encapsulation, water dispersion, bioaccessibility and bioactivities of curcumin, Food Hydrocolloids 105 (2020) 105821.

[7] J. Chen, F. Li, Z. Li, D.J. McClements, H. Xiao, Encapsulation of carotenoids in emulsion-based delivery systems: Enhancement of β-carotene water-dispersibility and chemical stability, Food Hydrocolloids 69 (2017) 49–55.

[8] S. Chen, N. Zhang, C.-H. Tang, Influence of nanocomplexation with curcumin on emulsifying properties and emulsion oxidative stability of soy protein isolate at pH 3.0 and 7.0, Food Hydrocolloids 61 (2016) 102–112.

[9] Chen, Y., & Ma, M. (2020). Foam and conformational changes of egg white as affected by ultrasonic pretreatment and phenolic binding at neutral pH. *Food Hydrocolloids*, *102*, 105568. http://doi.org/ 10.1016/j.foodhyd.2019.105568.

[10] Chumroenphat, T., Somboonwatthanakul, I., Saensouk, S., & Siriamornpun, S. (2021). Changes in curcuminoids and chemical components of turmeric (Curcuma longa L.) under freeze-drying and low-temperature drying methods. *Food Chemistry*, *339*, 128121. http://doi.org/ 10.1016/j.foodchem.2020.128121.

[11] J.H. Crowe, J.F. Carpenter, L.M. Crowe, The role of vitrification in anhydrobiosis, Annual Review of Physiology 60 (1998) 73–103, https://doi.org/10.1146/annurev.physiol.60.1.73.

[12] Dadi, D. W., Emire, S. A., Hagos, A. D., & Eun, J. (2020). Physical and Functional Properties, Digestibility, and Storage Stability of Spray- and Freeze-Dried Microencapsulated Bioactive Products from Moringa stenopetala Leaves Extract. *Industrial Crops and Products*, *156*, 112891. http://doi.org/ 10.1016/j.indcrop.2020.112891.

[13] F. Du, Y. Qi, H. Huang, P. Wang, X. Xu, Z. Yang, Stabilization of O/W emulsions via interfacial protein concentrating induced by thermodynamic incompatibility between sarcoplasmic proteins and xanthan gum, Food Hydrocolloids 124 (2022), 107242, https://doi.org/10.1016/j.foodhyd.2021.107242.

[14] Flamminii, F., Di Mattia, C. D., Nardella, M., Chiarini, M., Valbonetti, L., Neri, L.,... Pittia, P. (2020). Structuring alginate beads with different biopolymers for the development of functional ingredients loaded with olive leaves phenolic extract. *Food Hydrocolloids*, *108*, 105849. http://doi.org/ 10.1016/j.foodhyd.2020.105849.

[15] Gao, K., Zha, F., Yang, Z., Rao, J., & Chen, B. (2022). Structure characteristics and functionality of water-soluble fraction from high-intensity ultrasound treated pea protein isolate. *Food Hydrocolloids*, *125*, 107409. http://doi.org/ 10.1016/j.foodhyd.2021.107409.

[16] Geng, M., Wang, Z., Qin, L., Taha, A., Du, L., Xu, X.,... Hu, H. (2022). Effect of ultrasound and coagulant types on properties of β-carotene bulk emulsion gels stabilized by soy protein. *Food Hydrocolloids*, *123*, 107146. http://doi.org/ 10.1016/j.foodhyd.2021.107146.

[17] M.H. Grace, R.T. Hoskin, M. Hayes, M. Iorizzo, C. Kay, M.G. Ferruzzi, M.A. Lila, Spray-dried and freeze-dried protein-spinach particles; effect of drying technique and protein type on the bioaccessibility of carotenoids, chlorophylls, and phenolics, Food Chemistry 388 (2022), 133017, https://doi.org/10.1016/j.foodchem.2022.133017.

[18] Guo, P., Li, Y., An, J., Shen, S., & Dou, H. (2019). Study on structure-function of starch by asymmetrical flow field-flow fractionation coupled with multiple detectors: A review. *Carbohydrate Polymers*, *226*, 115330. http://doi.org/ 10.1016/j.carbpol.2019.115330.

[19] Q. Guo, J. Su, X. Shu, F. Yuan, L. Mao, J. Liu, Y. Gao, Fabrication, structural characterization and functional attributes of polysaccharide-surfactant-protein ternary complexes for delivery of curcumin, Food Chemistry 337 (2021) 128019.

[20] Hadidi, M., Boostani, S., & Jafari, S. M. (2022). Pea proteins as emerging biopolymers for the emulsification and encapsulation of food bioactives. *Food Hydrocolloids*, *126*, 107474. http://doi.org/ 10.1016/j.foodhyd.2021.107474.

[21] O.A. Higuera-Barraza, C.L. Del Toro-Sanchez, S. Ruiz-Cruz, E. Marquez-Rios, Effects of high-energy ultrasound on the functional properties of proteins, Ultrasonics Sonochemistry 31 (2016) 558–562, https://doi.org/10.1016/j.ultsonch.2016.02.007.

[22] H. Hu, J. Wu, E.C.Y. Li-Chan, L.e. Zhu, F. Zhang, X. Xu, G. Fan, L. Wang, X. Huang, S. Pan, Effects of ultrasound on structural and physical properties of soy protein isolate (SPI) dispersions, Food Hydrocolloids 30 (2) (2013) 647–655.

[23] Izutsu, K. (2018). Applications of Freezing and Freeze-Drying in Pharmaceutical Formulations. In M. Iwayainoue, M. Sakurai, & M. Uemura (Eds.)(pp. 371-383).

[24] W. Jia, D.S. Sethi, A.J. van der Goot, J.K. Keppler, Covalent and non-covalent modification of sunflower protein with chlorogenic acid: Identifying the critical ratios that affect techno-functionality, Food Hydrocolloids 131 (2022), 107800, https://doi.org/10.1016/j.foodhyd.2022.107800.

[25] S. Jiang, J. Ding, J. Andrade, T.M. Rababah, A. Almajwal, M.M. Abulmeaty, H. Feng, Modifying the physicochemical properties of pea protein by pH-shifting and ultrasound combined treatments, Ultrasonics Sonochemistry 38 (2017) 835–842, https://doi.org/10.1016/j.ultsonch.2017.03.046.

[26] M. Joshi, B. Adhikari, P. Aldred, J.F. Panozzo, S. Kasapis, Physicochemical and functional properties of lentil protein isolates prepared by different drying methods, Food Chemistry 129 (4) (2011) 1513–1522, https://doi.org/10.1016/j.foodchem.2011.05.131.

[27] S. Jun, M. Yaoyao, J. Hui, M. Obadi, C. Zhongwei, X. Bin, Effects of single- and dual-frequency ultrasound on the functionality of egg white protein, Journal of Food Engineering 277 (2020), 109902, https://doi.org/10.1016/j.jfoodeng.2020.109902.

[28] S. Khatoon, N. Kalam, M.F. Shaikh, M.S. Hasnain, A.K. Hafiz, M.T. Ansari, Nanoencapsulation of Polyphenols as Drugs and Supplements for Enhanc-ing Therapeutic Profile-A Review, Current Molecular Pharmacology 15 (1) (2022) 77–107, https://doi.org/10.2174/1874467214666210922120924.

[29] H. Lee, G. Yildiz, L.C. Dos Santos, S. Jiang, J.E. Andrade, N.J. Engeseth, H. Feng, Soy protein nano-aggregates with improved functional properties prepared by sequential pH treatment and ultrasonication, Food Hydrocolloids 55 (2016) 200–209, https://doi.org/10.1016/j.foodhyd.2015.11.022.
[30] L. Li, R. Cai, P. Wang, X. Xu, G. Zhou, J. Sun, Manipulating interfacial behavior and emulsifying properties of myosin through alkali-heat treatment, Food Hydrocolloids 85 (2018) 69–74, https://doi.org/10.1016/j.foodhyd.2018.06.044.
[31] Liu, B., & Zhou, X. (2015). Freeze-Drying of Proteins. In W. F. Wolkers & H. Oldenhof (Eds.), *Cryopreservation and Freeze-Drying Protocols*(pp. 459-476). Springer New York.
[32] Liu, B., & Zhou, X. (2021). Freeze-Drying of Proteins. In W. F. Wolkers & H. Oldenhof (Eds.), *Cryopreservation and Freeze-Drying Protocols*(pp. 683-702). Springer US.
[33] F. Liu, D. Ma, X. Luo, Z. Zhang, L. He, Y. Gao, D.J. Mcclements, Fabrication and characterization of protein-phenolic conjugate nanoparticles for co-delivery of curcumin and resveratrol, Food Hydrocolloids 79 (2018) 450–461, https://doi.org/10.1016/j.foodhyd.2018.01.017.
[35] Y. Liu, Z.Y. Zhang, L.D. Hu, High efficient freeze-drying technology in food industry, Critical Reviews in Food Science and Nutrition 62 (12) (2022) 3370–3388, https://doi.org/10.1080/10408398.2020.1865261.
[36] M. Mansour, M. Salah, X. Xu, Effect of microencapsulation using soy protein isolate and gum arabic as wall material on red raspberry anthocyanin stability, characterization, and simulated gastrointestinal conditions, Ultrasonics Sonochemistry 63 (2020) 104927.
[37] L. Mihalcea, V. Barbu, E. Enachi, D.G. Andronoiu, G. Râpeanu, M. Stoica, L. Dumitrașcu, N. Stănciuc, Microencapsulation of Red Grape Juice by Freeze Drying and Application in Jelly Formulation, Food Technology and Biotechnology 58 (1) (2020) 20–28.
[38] J. Pan, H. Lian, H. Jia, S. Li, R. Hao, Y. Wang, X. Zhang, X. Dong, Ultrasound treatment modified the functional mode of gallic acid on properties of fish myofibrillar protein, Food Chemistry 320 (2020) 126637.
[39] C. Pascal, C. Poncet-Legrand, A. Imberty, C. Gautier, P. Sarni-Manchado, V. Cheynier, A. Vernhet, Interactions between a non glycosylated human proline-rich protein and flavan-3-ols are affected by protein concentration and polyphenol/protein ratio, Journal of Agricultural and Food Chemistry 55 (12) (2007) 4895–4901, https://doi.org/10.1021/jf0704108.
[40] K. Ravichandran, R. Palaniraj, N.M.M.T. Saw, A.M.M. Gabr, A.R. Ahmed, D. Knorr, I. Smetanska, Effects of different encapsulation agents and drying process on stability of betalains extract, Journal of Food Science and Technology 51 (9) (2014) 2216–2221, https://doi.org/10.1007/s13197-012-0728-6.
[41] G. Ren, Y. He, C. Liu, F. Ni, X. Luo, J. Shi, Y. Song, T. Li, M. Huang, Q. Shen, H. Xie, Encapsulation of curcumin in ZEIN-HTCC complexes: Physicochemical characterization, in vitro sustained release behavior and encapsulation mechanism, Lwt-Food Science and Technology 155 (2022) 112909.
[42] X. Ren, C. Li, F. Yang, Y. Huang, C. Huang, K. Zhang, L. Yan, Comparison of hydrodynamic and ultrasonic cavitation effects on soy protein isolate functionality, Journal of Food Engineering 265 (2020), 109697, https://doi.org/10.1016/j.jfoodeng.2019.109697.
[43] S. Roy, R. Priyadarshi, P. Ezati, J.-W. Rhim, Curcumin and its uses in active and smart food packaging applications-a comprehensive review, Food Chemistry 375 (2022) 131885.
[44] Saqueti, B., Alves, E. S., Castro, M. C., Dos Santos, P., Sinosaki, N., Senes, C.,... Santos, O. O. (2021). Shelf Life of Bioactive Compounds from Acerola Pulp (Malpighia spp.) through Freeze-Drying and Microencapsulation. *Journal of the Brazilian Chemical Society*, *32*(10), 2009-2016. http://doi.org/10.21577/0103-5053.20210096.
[45] W.u. Shanshan, H. Meigui, L.i. Chunyang, C. Zhi, C. Li, H. Wuyang, L.i. Ying, F. Jin, Fabrication of ovalbumin-burdock polysaccharide complexes as interfacial stabilizers for nanostructured lipid carriers: Effects of high-intensity ultrasound treatment, Food Hydrocolloids 111 (2021) 106407.
[46] Y. Shen, X. Tang, Y. Li, Drying methods affect physicochemical and functional properties of quinoa protein isolate, Food Chemistry 339 (2021), 127823, https://doi.org/10.1016/j.foodchem.2020.127823.
[47] K.J. Siebert, N.V. Troukhanova, P.Y. Lynn, Nature of polyphenol-protein interactions, Journal of Agricultural and Food Chemistry 44 (1) (1996) 80–85, https://doi.org/10.1021/jf9502459.
[48] A. Tahir, R. Shabir Ahmad, M. Imran, M.H. Ahmad, M. Kamran Khan, N. Muhammad, M.U. Nisa, M. Tahir Nadeem, A. Yasmin, H.S. Tahir, A. Zulifqar, M. Javed, Recent approaches for utilization of food components as nano-encapsulation: a review, International Journal of Food Properties 24 (1) (2021) 1074–1096.
[49] K. Tanaka, T. Takeda, K. Miyajima, CRYOPROTECTIVE EFFECT OF SACCHARIDES ON DENATURATION OF CATALASE BY FREEZE-DRYING, Chemical & Pharmaceutical Bulletin 39 (5) (1991) 1091–1094.
[50] C. Tang, Nanocomplexation of proteins with curcumin: From interaction to nanoencapsulation (A review), Food Hydrocolloids 109 (2020), 106106, https://doi.org/10.1016/j.foodhyd.2020.106106.
[51] C. Tang, X. Wang, X. Yang, L. Li, Formation of soluble aggregates from insoluble commercial soy protein isolate by means of ultrasonic treatment and their gelling properties, Journal of Food Engineering 92 (4) (2009) 432–437, https://doi.org/10.1016/j.jfoodeng.2008.12.017.
[52] Tawalbeh, D., Ahmad, W. A. N. W., & Sarbon, N. M. (Effect of ultrasound pretreatment on the functional and bioactive properties of legumes protein hydrolysates and peptides: A comprehensive review. *Food Reviews International*. http://doi.org/10.1080/87559129.2022.2069258.
[53] C. Thongkaew, M. Gibis, J. Hinrichs, J. Weiss, Polyphenol interactions with whey protein isolate and whey protein isolate-pectin coacervates, Food Hydrocolloids 41 (2014) 103–112, https://doi.org/10.1016/j.foodhyd.2014.02.006.
[54] X. Tong, J. Cao, T. Tian, B.o. Lyu, L. Miao, Z. Lian, W. Cui, S. Liu, H. Wang, L. Jiang, Changes in structure, rheological property and antioxidant activity of soy protein isolate fibrils by ultrasound pretreatment and EGCG, Food Hydrocolloids 122 (2022) 107084.
[55] M. Volić, I. Pećinar, D. Micić, V. Đorđević, R. Pešić, V. Nedović, N. Obradović, Design and characterization of whey protein nanocarriers for thyme essential oil encapsulation obtained by freeze-drying, Food Chemistry 386 (2022) 132749.
[56] Waghmare, R. B., Choudhary, P., Moses, J. A., Anandharamakrishnan, C., & Stapley, A. (Trends in Approaches to Assist Freeze-Drying of Food: A Cohort Study on Innovations. *Food Reviews International*. http://doi.org/10.1080/87559129.2021.1875232.
[57] M. Wang, X. Chen, Y. Zou, H. Chen, S. Xue, C. Qian, P. Wang, X. Xu, G. Zhou, High-pressure processing-induced conformational changes during heating affect water holding capacity of myosin gel, International Journal of Food Science and Technology 52 (3) (2017) 724–732.
[58] Y. Wang, S. Wang, R. Li, Y. Wang, Q. Xiang, K. Li, Y. Bai, Effects of combined treatment with ultrasound and pH shifting on foaming properties of chickpea protein isolate, Food Hydrocolloids 124 (2022), 107351, https://doi.org/10.1016/j.foodhyd.2021.107351.
[59] Y. Wang, L. Zhang, P. Wang, X. Xu, G. Zhou, pH-shifting encapsulation of curcumin in egg white protein isolate for improved dispersity, antioxidant capacity and thermal stability, Food Research International 137 (2020), 109366, https://doi.org/10.1016/j.foodres.2020.109366.
[60] A. Wilkowska, W. Ambroziak, A. Czyzowska, J. Adamiec, Effect of Microencapsulation by Spray-Drying and Freeze-Drying Technique on the Antioxidant Properties of Blueberry (Vaccinium myrtillus) Juice Polyphenolic Compounds, Polish Journal of Food and Nutrition Sciences 66 (1) (2016) 11–16, https://doi.org/10.1515/pjfns-2015-0015.
[61] C. Wu, H. Dong, P. Wang, X. Xu, Y. Zhang, Y. Li, Insight into the effect of charge regulation on the binding mechanism of curcumin to myofibrillar protein, Food Chemistry 352 (2021), 129395, https://doi.org/10.1016/j.foodchem.2021.129395.
[62] C. Wu, L. Li, Q. Zhong, R. Cai, P. Wang, X. Xu, G. Zhou, M. Han, Q. Liu, T. Hu, T. Yin, Myofibrillar protein–curcumin nanocomplexes prepared at different ionic strengths to improve oxidative stability of marinated chicken meat products, LWT 99 (2019) 69–76.
[63] S. Yan, J. Xu, S. Zhang, Y. Li, Effects of flexibility and surface hydrophobicity on emulsifying properties: Ultrasound-treated soybean protein isolate, Lwt-Food Science and Technology 142 (2021) 110881.
[64] D. Yuan, F. Zhou, P. Shen, Y. Zhang, L. Lin, M. Zhao, Self-assembled soy protein nanoparticles by partial enzymatic hydrolysis for pH-Driven Encapsulation and Delivery of Hydrophobic Cargo Curcumin, Food Hydrocolloids 120 (2021), 106759, https://doi.org/10.1016/j.foodhyd.2021.106759.
[65] L.i. Zhang, J. Sun, Y. Qi, Y. Song, Z. Yang, Z. Li, L. Liu, P. Wang, X. Xu, G. Zhou, Forming nanoconjugates or inducing macroaggregates, curcumin dose effect on myosin assembling revealed by molecular dynamics simulation, Colloids and Surfaces a-Physicochemical and Engineering Aspects 607 (2020) 125415.
[66] L.i. Zhang, P. Wang, Z. Yang, F. Du, Z. Li, C. Wu, A. Fang, X. Xu, G. Zhou, Molecular dynamics simulation exploration of the interaction between curcumin and myosin combined with the results of spectroscopy techniques, Food Hydrocolloids 101 (2020) 105455.
[67] X. Zhang, Z. Zuo, W. Ma, P. Yu, T. Li, L. Wang, Assemble behavior of ultrasound-induced quinoa protein nanoparticles and their roles on rheological properties and stability of high internal phase emulsions, Food Hydrocolloids 117 (2021), 106748, https://doi.org/10.1016/j.foodhyd.2021.106748.
[68] Y. Zhang, E. Wright, Q. Zhong, Effects of pH on the Molecular Binding between beta-Lactoglobulin and Bixin, Journal of Agricultural and Food Chemistry 61 (4) (2013) 947–954, https://doi.org/10.1021/jf303844w.
[69] H. Zhao, Z. Ma, P. Jing, Interaction of soy protein isolate fibrils with betalain from red beetroots: Morphology, spectroscopic characteristics and thermal stability, Food Research International 135 (2020), 109289, https://doi.org/10.1016/j.foodres.2020.109289.